ChemComm

Standing, Lying, and Sitting: Translating Building Principles of the Cell Membrane to Synthetic 2D Material Interfaces

Journal:	*ChemComm*
Manuscript ID	CC-FEA-03-2018-002596.R1
Article Type:	Feature Article

Journal Name

ARTICLE

Standing, Lying, and Sitting: Translating Building Principles of the Cell Membrane to Synthetic 2D Material Interfaces

Received 00th January 20xx,
Accepted 00th January 20xx

DOI: 10.1039/x0xx00000x

www.rsc.org/

S.A. Claridge[a]

A striking number of problems in modern materials chemistry relate to controlling structure at scales 5-10 nm, important in applications ranging from nanoscale electronics to organic materials for energy conversion. Interfacial patterning is potentially valuable in establishing and stabilizing high-resolution structural features. While chemical patterning at such short length scales is unusually difficult using many traditional top-down approaches, it has been achieved with remarkable efficiency and chemical diversity in two seemingly unrelated areas: in the lipid bilayers that make up cell membranes, and in the noncovalent functionalization of 2D materials such as graphene. At the intersection of these two areas are lessons of significant utility for controlling synthetic material interface chemistry across a range of length scales.

Introduction. Controlling structure at 5-10 nm scales is central to many emerging areas of materials chemistry (Figure 1a), including nanoscale electronic devices[1-2] and organic materials for energy conversion.[3-4] High-resolution interfacial patterning (*e.g.* utilizing monolayer chemistry to create lines of functional groups), has the potential to create surfaces that would grow structural elements of organic and inorganic materials for these applications. However, techniques such as microcontact printing[5] that have been very successful in patterning monolayers at larger scales have not been straightforward to apply. In part, this is due to challenges in creating well-defined patterns in standing-phase monolayers at few-nm scales.

At the same time, high-resolution chemical patterns are central to biology, suggesting sets of design principles that can be translated to synthetic materials. For instance, the structure of the DNA double helix (diameter 2 nm, length 0.34 nm x # of bases), has been broadly leveraged to create discrete nanoscale structures in the form of DNA origami,[6] and as a recognition element to control crystallization of inorganic nanocrystals.[7] Likewise, peptides form structures (*e.g.* α helices and β sheets) with nm-scale chemical features that can template interactions with inorganic materials.[8]

Phospholipids, the primary constituents of the cell membrane (Figure 1b), typically contain two alkyl chains and four or more polar functional groups that control at sub-nm scales both the dielectric environment and chemical functionality available at the membrane periphery.[9] In contrast with DNA and peptides, which utilize a relatively limited set of building blocks (4 DNA bases, 20 amino acids), hundreds of structurally distinct lipids tailor the interfacial structure of the cell membrane using variations in headgroup chemistry and alkyl chains. The membrane leverages the structural complexity and controlled flexibility of lipids to control interactions between the cell and its environment at scales from <10 nm to multiple μm, suggesting the design of similarly sophisticated functionality for synthetic nanomaterials.

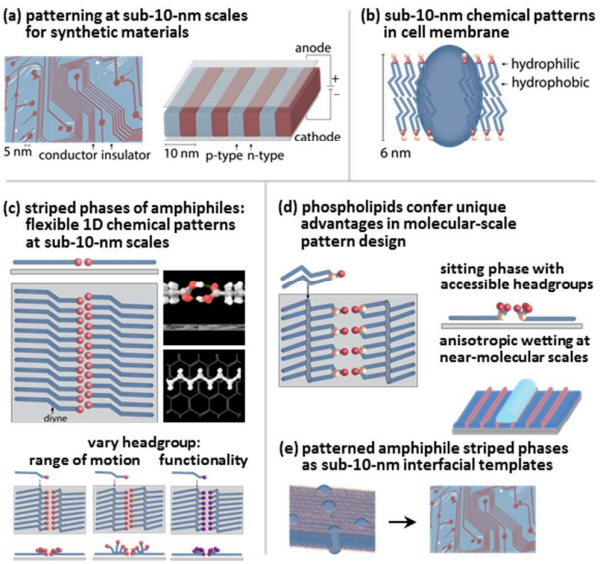

Figure 1. (a) Applications for controlled interface structure at sub-10-nm scales in synthetic materials. (b) Sub-10-nm chemical patterns in the cell membrane. (c) Striped phases of amphiphiles create 1D chemical patterns on synthetic materials. (d) Striped phospholipid 'sitting' phases leverage useful elements of biological flexibility and functionality. (e) Conversion of standing phase amphiphiles into striped interfacial templates.

[a] Department of Chemistry and Weldon School of Biomedical Engineering, Purdue University, West Lafayette, IN 47907

Many emerging synthetic material applications require ultranarrow (few-nm) 1D structures (*e.g.* circuit elements, Figure 1a), which would not be straightforward to create based on the 2D structure of the cell membrane. However, molecules similar to amphiphiles in the cell membrane can also form noncovalently adsorbed 'lying-down' phases on graphite, graphene, and other 2D materials[10-13] (Figure 1c,d). Such interfaces display, in essence, a repeating cross-section of a lipid bilayer; stripes of alkyl chains and functional headgroups alternate with a pitch 5-10 nm dictated by chain length, creating an 1D analog of the flexible molecular ordering in the cell membrane.

Studies of lying-down phases on 2D materials have been performed for many years at the solid–liquid interface with an organic solvent, or at the solid–gas interface.[11-13] The phenomenal resolution of scanning probe microscopy is leveraged to resolve molecular or sub-molecular details of both ordering and electronic structure.[14-16]

More recently, a growing body of work has begun to examine strategies for controlling interactions between the monolayer and its environment, including host-guest interactions and the growth of multilayer films,[17-21] as well as controlling wetting of 2D materials.[22-25] These goals require initial ordering to establish the monolayer structure, but often also a degree of controlled disordering, enabling functional groups in the monolayer to interact with their environment. In balancing order and flexibility, and in designing chemical structures that mediate transitions between two different chemical environments (*e.g.* a nonpolar 2D substrate and a polar solvent environment), there is much to be learned from biology. At the same time, the 1D structures in striped phases represent a fundamental departure from the chemistry of the cell membrane. Here, we provide a perspective bridging the literature on standing and lying-down phases of amphiphiles, and describing recent work in understanding the relationship between a noncovalently adsorbed striped monolayer and its environment.

Lying-down phases on 2D materials. Molecules with long alkyl chains have been known to selectively adsorb to carbon surfaces since at least the early 1950s.[26] Lying-down orientations for the chains were postulated as early as 1957,[27] based on the similarity between the C–C–C distance along the alkyl backbone (2.56 Å) and the distance between hexagonal centers in the graphite lattice (2.46 Å), as shown in Figure 2a. In the context of understanding lubrication, early calorimetry experiments established that not only graphite,[28] but also MoS_2 and WS_2 were capable of strongly adsorbing long hydrocarbons,[29] suggesting the likelihood of similar adsorbed structures, although epitaxial matching with the substrate lattice would be weaker (Figure 2b). Later, with the development of scanning tunneling microscopy (STM),[30] it became possible to directly observe the structures of lying-down phases,[31-32] and to elucidate differences in ordering based on the introduction of specific functional groups.[32-33] Early observations found that alkanes form striped lamellar phases, with stripe widths dependent on chain length. For alkanes with a functional headgroup, intermolecular distances along the lamellae depend on the relative size of the head and chain: for very small functional groups (*e.g.* –OH), chains can orient with the alkyl zig-zag perpendicular to the substrate, leading to interchain distances ~0.43 nm; for slightly larger headgroups (*e.g.* –COOH), the alkyl chain zig-zag lies parallel to the surface, leading to interchain distances ~0.47 nm.[32] Hydrogen bonding and other interactions between headgroups can also cause the alkyl chain to adopt different angles relative to the lamellar axis and/or change domain structure. Thus, similar to the cell membrane, a delicate balance of interactions between chains and headgroups determines layer structure.

Diynes as reactive building blocks for self-assembly. Many classes of lying-down molecular layers have been developed,[11-13,33-37] using structural motifs that encourage strong van der Waals interactions with the substrate (*e.g.* long alkyl chains, π systems) and/or stabilizing interactions with other molecules (*e.g.* H-bonding, covalent frameworks). Throughout this feature article, we will focus on noncovalent monolayers based on long-chain diynes,[38-40] which can be photopolymerized. Polymerization couples molecules within the noncovalent monolayer in ways that change electronic properties, stability, and perhaps more surprisingly, interactions with the environment. We start with a brief examination of the assembly of diynes in standing phases, highlighting the balance between order and disorder in determining reactivity and environmental interactions.

Like lying-down phases, reactivity of diynes in 3D crystals has been known since at least the 1950s.[41-42] The mechanism of polymerization of ordered diynes was studied in the 1970s by Wegner[43-44] and others,[44-45] leading to the understanding that the molecules can react to heat[46] or light,[43,47] forming a conjugated ene-yne polymer backbone through a diradical intermediate (Figure 3).

Both order and flexibility are integral to the polymerization. An increase of as little as 1 Å in the distance between bond-forming carbons can decrease polymerization rates by a factor of 2,[45,48] with the consequence that disordered molecules do not polymerize readily. At the same time, a small amount of flexibility is key — the diyne in the monomer must rehybridize to join the ene-yne polymer backbone, typically reorienting the flanking sections of the molecule and altering lattice structure.[44-45,49]

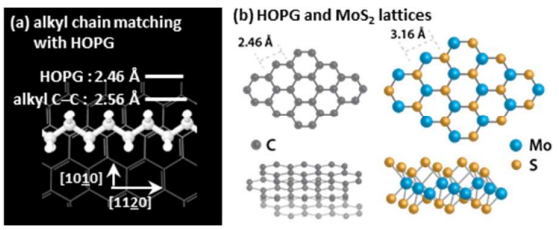

Figure 2. Illustrations of (a) structural matching between alkyl chain and highly oriented pyrolytic graphite (HOPG) lattice that leads to formation of lying-down phases, and (b) lattice structures of HOPG and MoS_2.

Structural flexibility also impacts physical properties after polymerization. Electronic delocalization along the ene-yne changes optical absorption and emission spectra vs those of the monomer.[50-51] Initially, polymerization produces a slightly strained form of the ene-yne with an absorbance maximum around 640 nm, which appears blue. In response to heat, the polymer can undergo a thermochromic transition, relaxing into a form in which periodic twisting of the polymer backbone reduces conjugation length; this form has an absorbance maximum near 500 nm, and appears red.

As understanding of the polymerization process increased, further studies by Ringsdorf and others demonstrated that it was feasible to polymerize diynes ordered in Langmuir films,[44,52-53] where again the degree of ordering played a significant role in polymerization. In this way, it was possible both to stabilize thin molecular layers, and to use the thermochromic transition as a basis for sensing environmental stimuli that change headgroup orientation (*e.g.* binding of metal ions or other charged species).[54]

In the early 1980s, multiple reports of diyne phospholipids emerged.[55-57] These aimed at stabilizing biocompatible surfaces and liposomes,[53,55-56] but also at creating photographic emulsions at Eastman Kodak,[57-58] hinting at the broad utility of these molecules in material design.

Lying-down phases of diynes. As lying-down phases were studied at molecular scales by STM, monolayers of diynes began to draw significant interest.[38-40,59] In lying-down phases, aligned diynes can still be polymerized by UV irradiation, but can also be polymerized by tunneling electrons from an STM tip. Electronic delocalization in the resulting ene-yne facilitates tunneling, making it possible to observe formation of individual polymers in the STM. Individual polymers can extend the entire length of a molecular domain (> 100 nm); however, both inelastic electron tunneling spectroscopy and theory suggest the HOMO-LUMO gap for oligomers with lengths ≥10 nm are essentially the same.[60]

Even in 2D lying-down phases, structural flexibility is important in the polymerization process. In order for the ene-yne to remain in the plane of the monolayer, the flanking alkyl chain segments must tilt relative to the lamellar axis (Figure 3). Molecular models suggest that steric clashes between tilted and untilted chain segments become significant for segmental lengths >8 carbons.[61] If tilting of the alkyl chains is unfavorable, lifting the ene-yne and adjacent methylene groups ~1.4 Å above the plane of the monolayer satisfies bond angle requirements. For 10,12-PCDA, the most widely used commercially available diynoic fatty acid, long alkyl chain segments lead to a lifted configuration for the polymer backbone.[39-40] Rates of polymerization for surface templated diacetylene monolayers are typically substantially lower than for solid-state polymerization.[62-63]

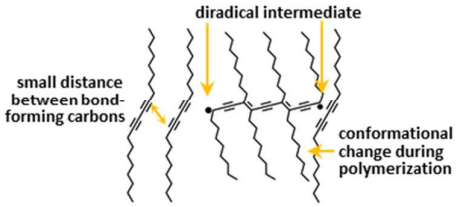

Figure 3. Order and flexibility in diyne polymerization.

Interactions with the substrate are also important in polymerization and subsequent use. For monolayers of diynoic acids on MoS_2, epitaxy with the substrate is weaker than for monolayers on HOPG, with higher rates of diyne polymerization.[62,64] Adsorbates alter the electronic structure of the substrate to varying degrees, and striped patterns of specific functional groups (*e.g.* amines) have been used to modulate charge carrier density in graphene and MoS_2.[13,15-16]

When monolayers are assembled from nonpolar solvents, interactions between polar headgroups are frequently strong enough to retain the headgroup in the plane of the monolayer (~15 kcal/mol for COOH dimers, based on formic acid[65]). However, use of headgroups as functional patterns at the interface would require that they be accessible to the environment, implying some range of motion of the functional head. This flexibility of the headgroup may determine not only where it can interact with the environment (*e.g.* to capture an analyte from solution), but also its chemistry, based on the local dielectric environment near the interface.

Previous work by Whitesides and others found pronounced differences in the behaviour of functional groups at polar–nonpolar boundaries at the periphery of standing phase self-assembled monolayers (SAMs).[66-68] For instance, the $pK_{1/2}$ values (the point at which half the functional groups are ionized) for carboxylic acids varied from 8 (for 100% COOH-terminated monolayers) to 11 (for monolayers with only 15% COOH termination). This behaviour was rationalized in terms of the limited ability of the nonpolar monolayer interior to stabilize the charged form of the functional group. Measurements by Latour and coworkers showed that while the $pK_{1/2}$ of COOH groups shifts up, the value for NH_2 groups shifts down,[68] reflecting a similar restriction in the ability to ionize in the dielectric environment at the interface.

In contrast with the 2D assembly of functional groups at the periphery of a standing phase SAM, headgroups in lying-down phases form 1D assemblies within the predominantly nonpolar monolayer, potentially further restricting the ability to ionize. At the same time, the noncovalent molecule–substrate interaction suggests the possibility of flexible positioning of functional groups to adjust local dielectric.

Below, we will discuss experimental and theoretical findings relating to ionization and other chemical characteristics of lying-down phases impacted by flexibility and the positioning of polar functional groups at polar–nonpolar boundary. First we provide brief context for these questions, based on the structure and function of the phospholipid architecture at a biological polar–nonpolar interface.

A biological approach to structuring interfaces. The phospholipid structure provides a remarkable means of establishing distinct chemical environments in the membrane periphery (Figure 4a). For single-chain amphiphiles, the

footprint of the alkyl chain (~20–25 Å^2) restricts the range of headgroups that can be attached without impacting chain packing; this is true for both standing and lying-down phases (Figure 4b, top left). In contrast, the larger footprint of the two phospholipid alkyl chains (~40–50 Å^2) establishes additional space for bulky functional groups (*e.g.* phosphate, choline) in the polar membrane periphery, and to provide conformational flexibility to smaller ones (*e.g.* primary amines). These properties are important in directing interactions with the environment, both in multivalent binding, and in reorienting headgroup dipoles (Figure 4b, bottom left).[69]

As discussed above, ionizable functional groups (*e.g.* weak acids and bases) at a nonpolar interface experience restrictions in their ability to ionize. Managing the transition from nonpolar membrane interior to polar periphery, the phospholipid headgroup (Figure 4a) utilizes polar ester linkages, a phosphate group (which has a very low native pK_a), and typically a short, flexible alkyl linkage to an amine. The phosphate is asymmetrically mounted on a 3-carbon glycerol backbone (highlighted in yellow); shifts in positions of the nonpolar alkyl chains connected to the other two glycerol carbons can thus reorient the phosphate and other functional groups in the head. Overall, the headgroup architecture enables a broad range of chemistry to occur directly adjacent to the nonpolar membrane interior, suggesting the possibility of similar impacts at nonpolar 2D material interfaces.

Transmembrane proteins and other structures that transect the bilayer are strikingly sensitive to its hydrophobic cross-sectional width.[9,70] A mismatch of as little as a few atomic diameters between the local hydrophobic cross-section of the membrane and an embedded structure (Figure 4b, top right) is enough to cause a preference for another section of the membrane.[71] More specific chemical interactions with lipid headgroups and alkyl chains also stabilize some membrane proteins.[72] A phenomenon known as lysine snorkelling[73] illustrates this principle (Figure 4b, bottom right). The lysine amino acid side chain comprises a four-carbon flexible alkyl chain terminating in a primary amine. Structures such as apolipoprotein helices that thread the polar–nonpolar boundary of the membrane position the peptide backbone of a lysine residue in the nonpolar membrane interior; the amine, on its flexible alkyl linker, 'snorkels' up to dock next to

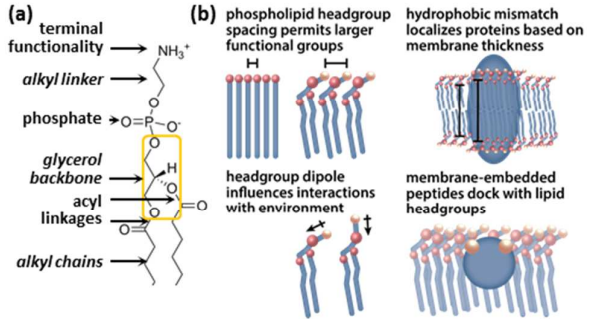

Figure 4. (a) Structural elements of a phospholipid, and (b) their roles in a cell membrane, supporting structures of complex molecules such as transmembrane proteins.

negatively charged phosphates in the membrane periphery, setting the height of the helix in the membrane, much like floating a boat. Similar flexibility could be envisioned to be useful in docking structures to a 2D material surface.

Taken together, these ideas illustrate ways in which cells use the difference between hydrophilic and hydrophobic sections of amphiphiles, controlled structural flexibility, and the specific structures of phospholipid heads and tails to control interactions with their environment. Below, we discuss ways in which these principles can control interactions between synthetic 2D materials and their environment.

Using phospholipids to functionalize 2D materials. Like long-chain carboxylic acids (Figure 5a,b), phospholipids can also assemble into striped phases on 2D materials (Figure 5c,d) when deposited from organic solvents or by Langmuir-Schaefer transfer.[22] Figure 5 illustrates the monolayer structure formed by a commercially available diyne phospholipid, 1,2-bis(10,12-tricosadiynoyl)-*sn*-glycero-3-phosphocholine (diyne PC). Energy-minimized molecular models (Figure 5c) suggest that phospholipids adsorb with the phosphate adjacent to the HOPG, and the terminal amine projecting at the environmental interface. We refer to the resulting monolayer structure as a 'sitting' phase, in contrast with a true 'lying-down' phase, highlighting the difference in headgroup orientation. Monolayers of diyne phospholipids can be photopolymerized by UV irradiation, similar to diynoic acids. Because the monomer has two alkyl chains per

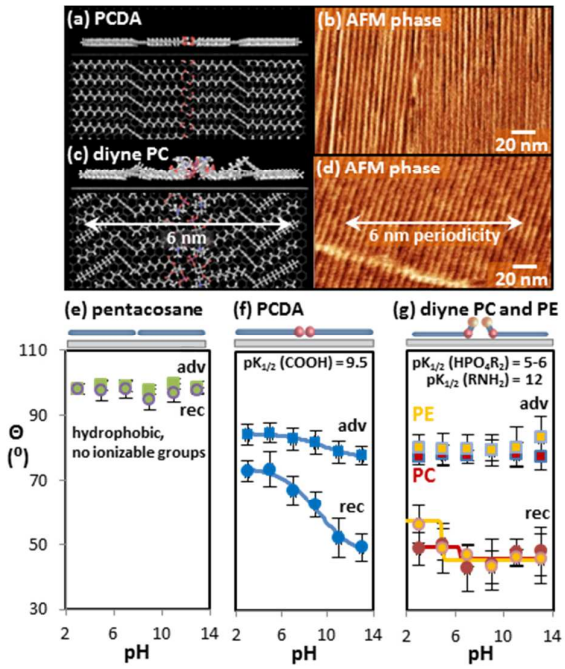

Figure 5. Molecular models and AFM images of of (a,b) lying-down phase of 10,12-PCDA and (c,d) sitting phase of diyne PC on HOPG. Advancing (adv) and receding (rec) contact angle titrations for lying-down phases of (e) pentacosane, (f) 10,12-PCDA, and (g) sitting phases of diyne PC and diyne PE. Adapted from Ref 22 with permission.

headgroup, lateral spacing between amines is ~1 nm; the lamellar pitch is ~6 nm, similar to 10,12-PCDA.

Interactions between a noncovalent monolayer and its environment. Although only 10-15% of the surface of such lamellar phases is comprised of polar headgroups, they exert a substantial influence on interfacial wetting, an ensemble measurement of interactions between the monolayer and the environment. Contact angle titrations using droplets of aqueous buffers enable measurement of the ionization behaviour of functional groups in the monolayers. For molecules lacking ionizable functional groups (*e.g.* pentacosane, Figure 5e), the angle between the substrate and the line tangent to a buffer droplet remain similar for droplets of acidic and basic buffers. As carboxylic acid groups in monolayers of 10,12-PCDA are ionized (Figure 5f), the surface becomes more hydrophilic, and the contact angle decreases. Based on the midpoint of the contact angle titration curve, the $pK_{1/2}$ of COOH groups in lying-down phases of 10,12-PCDA is ~9.5, a shift of ~5 units in comparison with ionization of acetic acid in dilute aqueous solution.

Sitting phases exhibit related but different wetting behavior (Figure 5g). The phosphate, positioned next to the nonpolar interface, undergoes a $pK_{1/2}$ shift similar to that experienced by the COOH group in lying-down phases of 10,12-PCDA. In contrast, the terminal primary amine in monolayers of diyne phosphoethanolamine (diyne PE) retains its solution ionization behavior, which is reasonable given its access to the polar solvent environment. Additionally, the phosphate retains a charge across much of the tested pH range, and lies between the amine and the nonpolar HOPG.

While the sitting phase geometry in phospholipids directly elevates the terminal functional group above the interface, the noncovalent molecule–substrate interaction in a lying-down phase also allows headgroups on single-chain amphiphiles to undergo excursions into the solvent. Even small changes in monolayer structure can alter this behaviour in useful ways.

For instance, conformational changes during polymerization can be exploited to make headgroups more available to the environment, based on the position of the polymerizable group (Figure 6). Lying-down monolayers of 10,12- and 4,6-PCDA (Figure 6a,b) exhibit similar contact angle curves prior to polymerization (Figure 6c, empty blue squares (10,12-PCDA) and empty gold squares (4,6-PCDA)), which is reasonable given their identical fractions of hydrophilic (f_{COOH}) and hydrophobic (f_{alkyl}) chemistry; calculated contact angles using the Young-Dupré equation for heterogeneous surfaces[74] (here, comprising alkyl and COOH components):

$$(1 + cos\ \theta_{PCDA})^2 = f_{alkyl}(1 + cos\ \theta_{alkyl})^2 + f_{COOH}(1 + cos\ \theta_{COOH})^2$$

should produce similar values for $\theta_{10,12\text{-PCDA}}$, $\theta_{4,6\text{-PCDA}}$, $\theta_{poly\text{-}10,12\text{-PCDA}}$, and $\theta_{poly\text{-}4,6\text{-PCDA}}$, if all monolayers adopt a similar lying-down structure. In contrast, after polymerization, both monolayers become somewhat more hydrophilic, but the increase in hydrophilicity (decrease in contact angle) is substantially more pronounced for 4,6-PCDA.

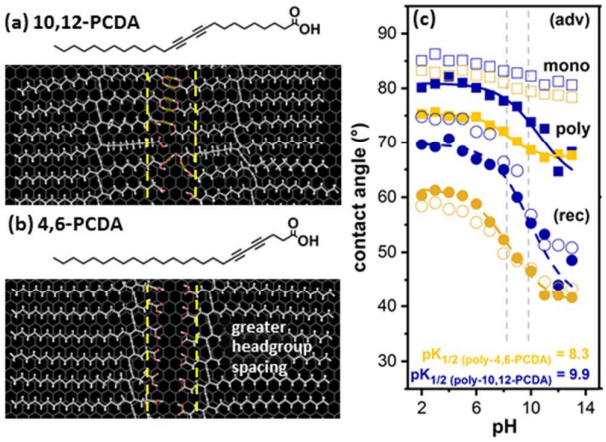

Figure 6. Models of polymerized monolayers of (a) 10,12-PCDA, and (b) 4,6-PCDA. (c) Advancing (adv) and receding (rec) contact angle titrations for 10,12-PCDA (blue) and 4,6-PCDA (gold) monolayers on HOPG, before (empty symbols) and after (filled) polymerization. Adapted from Ref 23 with permission.

These increases in hydrophilicity appear to arise from breakage of COOH headgroup dimers during polymerization (Figure 6a,b). Rehybridization of the diyne to form the ene-yne polymer backbone slightly narrows lamellae, requiring one of the conjoined alkyl chain segments to shift relative to the graphite lattice. Shifts in the segment bound to the COOH group can break COOH dimers, making headgroups more available to the solvent. Calculations suggest that in the case of 4,6-PCDA, relatively weak intermolecular interactions for the very short alkyl chain segment between the diyne and the COOH headgroup[65,75] cause this segment to shift, rather than the much longer 18-carbon terminal alkyl chain (Figure 6b). In 10,12-PCDA, segmental interaction strengths are more similar (Figure 6a), suggesting either end of the molecule may shift. These relationships are consistent with molecular dynamics simulations in which polymerization breaks the large majority of COOH dimers for 4,6-PCDA, while the majority of COOH dimers for 10,12-PCDA remain intact.

Striped wetting of striped monolayers. The striped amphiphilic structure of the surface suggests the possibility of generating wetting anisotropy at near-molecular scales, prototyping the ability to pattern interfaces at sub-10-nm scales. Earlier work by Whitesides[76] and others[77-78] demonstrated that striped functional patterns on surfaces (*e.g.* patterns of COOH-terminated molecules in CH_3-terminated standing phase SAMs) generates wetting anisotropy at larger scales, producing rodlike liquid droplets. At the same time, generating additional free surface area on a liquid droplet is energetically unfavorable, suggesting the need for strongly wetting chemistry (*e.g.* protruding ridges of charged diyne PC headgroups) to create directionality at very small scales.

The difference in headgroup chemistry between lying-down phases of 10,12-PCDA and sitting phases of diyne PC produces substantial differences in nanoscopic wetting.[24]

Figure 7 illustrates results of spraying nanoscale liquid droplets (1% glycerol in deionized water) at template surfaces of 10,12-PCDA (Figure 7a) and diyne PC (Figure 7b–e). On 10,12-PCDA templates, droplets localize predominantly at step edges in the HOPG (Figure 7a), suggesting weak interactions with the dimerized COOH headgroups on the timescale of droplet impact with the surface. In contrast, droplets sprayed at diyne PC surfaces adhere across the entire surface (Figure 7b), consistent with the electrostatic polarization and topographic protrusion of diyne PC headgroups (Figure 7b, inset).

Under normal laboratory environments, both headgroup chemistries produce spherical cap droplets. However, increasing environmental humidity in the spray chamber decreases droplet viscosity on impact, which can begin to induce nanoscopic directional wetting. At relative humidity (r.h.) levels >80%, droplets adopt a thin film morphology on impact (thickness ~5 nm, Figure 7c), and above 90% r.h., linear edges appear (Figure 7d,e). In some cases (e.g. Figure 7e), the liquid resolves into a series of rodlike features around the edge of the impact site, reflecting the stripe direction of the template (highlighted with arrows in Figure 7e). Populations of narrow rods with widths of ~6 and ~12 nm (Figure 7f) suggest liquid spreading along stripes of headgroups, pointing to the

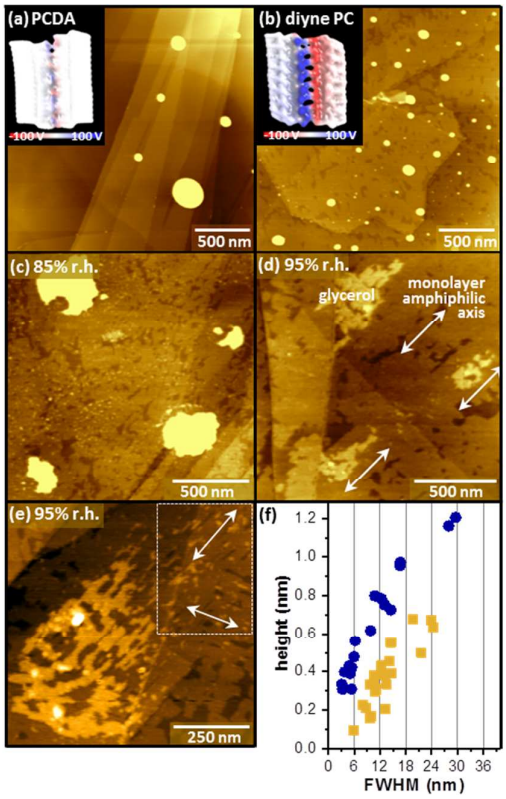

Figure 7. AFM images of nanoscale droplet adhesion to monolayers of (a) 10,12-PCDA, and (b-e) diyne PC (electrostatic surface maps of monolayers, insets a-b), at (b) 65% r.h., (c) 85% r.h., (d,e) 95% r.h. (f) Liquid rod widths and heights in areas similar to (e) illustrating that rod widths reflect template pitch. Adapted from Ref 24 with permission.

capability to use rows of phospholipid headgroups for interfacial patterning.

Controlling long-range ordering in noncovalent monolayers through Langmuir-Schaefer conversion. Controlling long-range ordering, either to create very large molecular domains, or to create specific patterns of functionality, represents a significant goal in noncovalent functionalization using striped phases. For standing phase SAMs, thermal annealing is commonly utilized to increase ordered domain size,[79] and microcontact printing facilitates generation of microscale functional patterns.[5,80] For lying-down phases, approaches based on flow and/or solvent annealing can enable long-range alignment.[81-82] Ordered molecular films can also be created on an aqueous subphase and transferred to a solid support by either vertical dipping (Langmuir-Blodgett, LB, transfer[83]) or horizontal dipping (Langmuir-Schaefer, LS, transfer[84]), as shown in Figure 8. Under appropriate transfer conditions, molecules retain their original orientation and ordering,[85] enabling molecular pattern transfer for standing phases.[86]

LS transfer also potentially represents a means of pre-assembling microscale patterns on an aqueous subphase and converting them into striped phases on a 2D material (Figure 8b). Early STM studies demonstrated nanoscale domain assembly on HOPG by LS transfer, with edge lengths up to ~100 nm.[22,24,38-39] Creating multi-µm domains or patterns via LS transfer is also possible, but requires increased control.

Again, water plays an important role. While HOPG is not typically considered to be especially hydrophilic, a growing body of work indicates that freshly cleaved graphite (or freshly synthesized graphene) has a relatively low water contact angle (~64° for freshly cleaved HOPG), which rises rapidly (~91° for HOPG aged 24 hours), due to adsorption of atmospheric contaminants.[87] Condensation of water on HOPG prior to the contact with the Langmuir film appears to decrease transfer efficiency (Figure 8c). A custom-built heated dipper (Figure 8d) enables substrate temperature control to limit condensation.[88]

Pre-heating the substrate and allowing it to cool rapidly on the subphase increases transfer ratios in comparison with room-temperature transfer, but also results in significant transfer of (typically unwanted) standing phases. In contrast, transfer with the HOPG maintained at 50–70 °C for 1–5 minutes routinely produces domains with edge lengths >10 µm for diyne PE (Figure 8e). At such scales, molecular alignment is visible based on small cracks that form in the monolayer as the lamellae narrow during polymerization (inset). Domain sizes for drop-casting with thermal annealing for the same molecule can be on the order of 1 µm, but variations in solute concentration as the solvent front recedes across the substrate typically produce uncontrolled vacancies and multilayers.

Large domains appear to increase stability toward solvents. Figure 8f and g illustrate the results of washing monolayers transferred at room temperature (Figure 8f) or 70 °C (Figure 8g). After vigorous washing with ethanol for 30 s, >98% of the monolayer remains intact on the annealed surface. This increased stability toward washing is consistent across

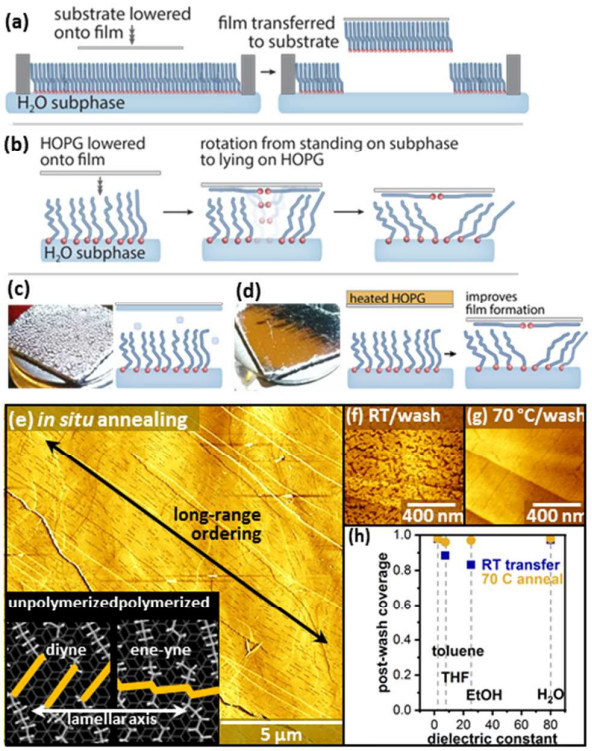

Figure 8. (a) LS transfer of standing phase and (b) conversion to lying-down phase. (c,d) Heated transfer stage improves transfer of lying-down phases. (e) Diyne PE transferred with *in situ* annealing at 70 °C for 4 min. Arrow highlights molecular alignment, visualized by polymerization-induced cracking defects (inset). Diyne PE films prepared through (f) room temperature and (g) annealed LS transfer, after washing with ethanol. (h) Surface coverage in polymerized diyne PE films after washing. Adapted from Ref. 88 with permission.

solvents with a range of polarities (Figure 8h), suggesting that subjecting such films to solution processing is reasonable.

Transferring molecular patterns via LS conversion. Creating specific patterns of molecules in noncovalent functionalization is also an important goal, enabling structured interactions with the environment. Conventional LS transfer lifts molecules from the interface in their original orientation (Figure 8a), and benefits from tightly-packed monolayers.[85] In contrast, conversion of a standing phase to a lying-down phase (Figure 8b) requires molecules to reorient substantially. Thus, parameters that optimize conversion to lying-down phases differ from those for direct transfer of standing phases.

In transfer from a standing phase environment in the Langmuir film to form a lying-down phase on HOPG, molecules that are strongly stabilized in the Langmuir film experience a greater energetic barrier to transfer. When Langmuir films of PCDA with both ordered (condensed) domains and disordered (expanded) domains are assembled on water, and molecules are then transferred to HOPG, SEM images of the transferred PCDA (Figure 9a) exhibit arrays of dark circular features on a bright background. These circular features are consistent with

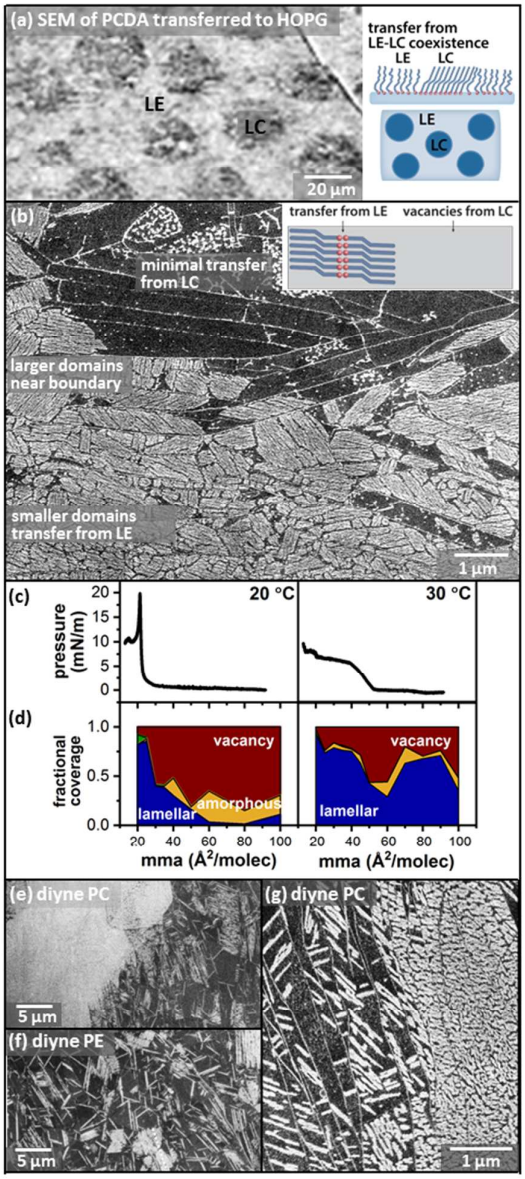

Figure 9. (a,b) SEM images of PCDA transferred to HOPG from Langmuir film containing disordered liquid expanded (LE) and ordered liquid condensed (LC) regions. (c,d) Isotherms and comparison of transfer at 20°C (left) and 30 °C (right). (e-g) domains (dark area near top of image), with small domains assembled over expanded phase regions in the Langmuir film. SEM images of diyne PC (e,g) and diyne PE (f) transferred to HOPG. Adapted from Ref. 89 and 90 with permission.

SEM images acquired at the boundaries of such vacancies (Figure 9b) show limited transfer from condensed phase. Local differences in mean domain sizes (*i.e.* large ordered domains near boundary vs smaller domains near bottom of image) are likely influenced by local differences in transfer rates. Based on previous studies of submonolayer island nucleation and growth,[91] the number density of domains, N, varies with the molecular adsorption rate (F), and the rate of molecular diffusion across the substrate (D), with

$$N \propto \left(\frac{F}{4D}\right)^{1/3}$$

In relation to this model, a fourfold difference in domain number density could indicate up to a 64-fold difference in local molecular transfer rates near the expanded–condensed boundary and in the bulk expanded phase, in the SEM image shown in Figure 9b. Overall, transfer of molecules that order into lamellar domains decreases for Langmuir films compressed to lower mean molecular areas (mma) (Figure 9c,d) or lower subphase temperatures (20 °C vs. 30 °C). Comparing transfer characteristics of structurally different single-chain amphiphiles and phospholipids (Figure 9e-g) reveals that molecules such as diyne PE or single-chain amides that can form stable hydrogen-bonding networks in the Lanmguir film undergo less facile transfer.[90]

A nondestructive spectroscopic probe of ordering in lying-down noncovalent monolayers. While SEM imaging is useful for visualizing domain structure, molecular orientation, and spatial patterning, in some applications, a nondestructive means of probing monolayer ordering over large areas is also useful. Polarization-modulated infrared reflection absorption spectroscopy (PM-IRRAS) has been used previously to examine ordering in standing phase monolayers (*e.g.* alkanethiols on Au(111)).[92] The technique proves to be useful in distinguishing alkyl chain ordering for lying-down monolayers as well (Figure 10).[25]

The PM-IRRAS measurement compares relative absorbance of components of an IR beam parallel and perpendicular to the plane of incidence, and therefore can be sensitive to the orientation of functional groups at an interface.[93] For lying-down alkyl chains with the zig-zag carbon backbone oriented parallel to the surface, the CH_2 asymmetric stretch dipole orients approximately normal to the interface (Figure 10a), leading to a strong peak in the PM-IRRAS spectrum (Figure 10c); a broader distribution of orientations for disordered chains (Figure 10b) leads to a weaker signal (Figure 10d). Correlating PM-IRRAS signal intensity with SEM imaging enables assessment of the overall degree of order (Figure 10e) or disorder (Figure 10f) of monolayers on graphene. The ratio between CH_2 asymmetric stretch intensity, $I(CH_{2a})$, and the CH_3 asymmetric stretch intensity, $I(CH_{3a})$, provides a useful discriminator between monolayers that exhibit predominantly ordered and disordered coverage (Figure 10g).

Conclusions

Many years of work have elucidated molecular design principles for inducing and characterizing order in noncovalently adsorbed monolayers on 2D materials.[11-13] Molecule–substrate interactions have been examined in detail, to understand Moire patterns and other features observed in STM images,[32] and to modulate 2D material electronic structure.[16] Likewise, molecule–molecule interactions ranging from hydrogen bonding[94-95] to the formation of covalent structures[37,40] have been examined for applications such as molecular electronics.

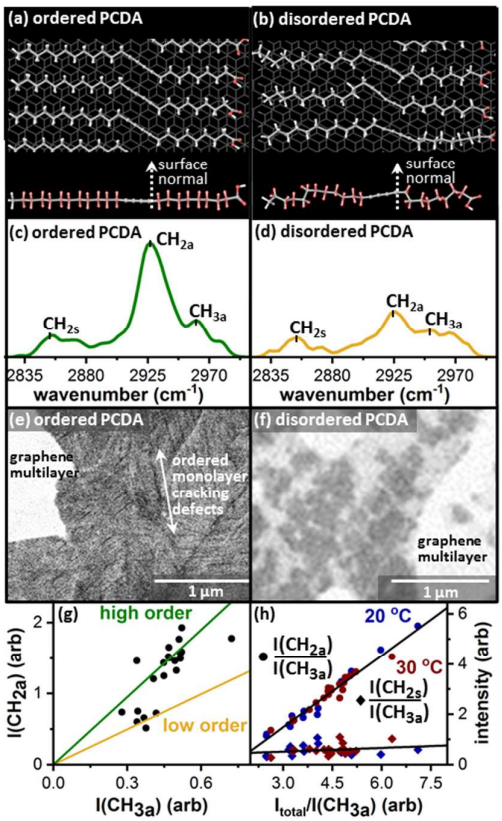

Figure 10. Molecular models of (a) ordered and (b) disordered monolayers of PCDA (CH_2 asymmetric stretch dipoles highlighted in red in side views). (c-f) Representative PM-IRRAS spectra (c,d) and SEM images (e,f) for ordered and disordered monolayers on graphene. (g) Ratio of $I(CH_{2a})/I(CH_{3a})$ discriminates between high (green) and low (gold) degrees of order. (h) CH_2 symmetric stretch does not predict ordering. Adapted from Ref. 25 with permission.

An equally strong understanding of the interactions between the monolayer and its environment can ultimately transform the 2D monolayer into a molecular foundation for 3D nanoscopic design. Developing this understanding presents significant, though tractable, challenges.

One such challenge involves understanding and controlling the positions of functional groups that are not tightly packed against the substrate basal plane. Part of the reason that so much is known about the structure of noncovalent monolayers is that it is often possible to resolve positions of individual methylene groups and other functional groups by STM.[11] Using functional groups in the monolayer to pattern interactions with the environment implies the need for flexibility; as a consequence, such monolayers are often more difficult to image using scanning probes. While techniques such as SEM imaging,[89] PM-IRRAS spectroscopy,[25] contact angle titrations[22-23] and frictional measurements[21] provide insight into certain aspects of the interface structure and chemistry, more structural information would clearly be useful.

Theoretical calculations can provide significant insights, but require the use of explicit solvents and other computationally

expensive elements, since hydrogen-bonding and other interactions with solvents are almost certain to be important.[96] In our own calculations, we find that the presence of even a small amount of explicit water in the region around the headgroups impacts interfacial behavior, suggesting the important role environmental humidity is likely to play at such interfaces.

Much as in the cell membrane, exact positioning of functional groups next to a nonpolar interface changes their chemistry.[22-23] Oriented dipoles are known to be important in further self-assembly at the interface,[97-98] which is likely to be especially important for polyfunctional headgroups such as those of phospholipids.[69] More broadly, this raises questions about designing interfaces that create 1D polar–nonpolar boundaries. To what extent do the phospholipid headgroup architectures that produce 2D polar–nonpolar boundaries create useful 1D dielectric environments? Are they equally useful in nonpolar solvent environments?

While the majority of the literature on 2D monolayers to date has focused on relatively small areas of the surface, controlling and patterning larger areas of the surface would also be essential for most practical applications. A number of approaches, such as those based on solvent flow, have been successful in this regard.[82] Langmuir-Schaefer protocols can further be utilized to create either large ordered domains or molecular patterns including vacancies.[88-89] Importantly, large ordered domains increase solvent stability, relevant to solution processing. Ultimately, such molecular patterns, perhaps consisting of many different types of molecules, can be designed and used across a range of scales. Specific nanoscopic patterns can be designed with resists that are removed to reveal areas of a surface on which molecules can assemble;[99] transfer from multi-component Langmuir films may ultimately enable spatial control over complementary length scales.

Such approaches set the stage for controlling interactions between a substrate and its environment across scales from <10 nm to mm. Stable lying-down phases such as polymerized phospholipids have broad potential to act as scaffolds for growing 3D nanostructures; the phospholipid headgroup in particular suggests design principles for creating distinct chemical environments over extremely short length scales for controlling structural growth exhibiting chemical diversity mirroring that observed in the cell membrane.

Conflicts of interest

There are no conflicts to declare.

Acknowledgements

SAC acknowledges support through an NSF CAREER award, NSF-CHE 1555173, a DuPont Young Professor Award, and a 3M Non-Tenured Faculty Award.

Notes and references

1 Asenov, A.; Kaya, S.; Brown, A. R., Intrinsic Parameter Fluctuations in Decananometer MOSFETs Introduced by Gate Line Edge Roughness. *IEEE Trans. Electron. Devices* **2003,** *50*, 1254-1260.

2 Shin, C., State-of-the-Art Silicon Device Miniaturization Technology and Its Challenges. *IEICE Electr. Expr.* **2014,** *11*, 1-11.

3 Perepichka, I. F.; Perepichka, D. F., *Handbook of Thiophene-Based Materials: Applications in Organic Electronics and Photonics*. Wiley: Chichester, United Kingdom, 2009.

4 Ostroverkhova, O., Organic Optoelectronic Materials: Mechanisms and Applications. *Chem. Rev.* **2016,** *116*, 13279-13412.

5 Xia, Y. N.; Whitesides, G. M., Soft Lithography. *Annu. Rev. Mater. Sci.* **1998,** *28*, 153-184.

6 Torring, T.; Voigt, N. V.; Nangreave, J.; Yan, H.; Gothelf, K. V., DNA Origami: A Quantum Leap for Self-Assembly of Complex Structures. *Chem. Soc. Rev.* **2011,** *40*, 5636-5646.

7 Macfarlane, R. J.; Lee, B.; Jones, M. R.; Harris, N.; Schatz, G. C.; Mirkin, C. A., Nanoparticle Superlattice Engineering with DNA. *Science* **2011,** *334*, 204-208.

8 Whaley, S. R.; English, D. S.; Hu, E. L.; Barbara, P. F.; Belcher, A. M., Selection of Peptides with Semiconductor Binding Specificity for Directed Nanocrystal Assembly. *Nature* **2000,** *405*, 665-668.

9 Luckey, M., *Membrane Structural Biology: With Biochemical and Biophysical Foundations*. 2nd ed.; Sheridan: U.S.A., 2014.

10 Giancarlo, L. C.; Flynn, G. W., Scanning Tunneling and Atomic Force Microscopy Probes of Self-Assembled, Physisorbed Monolayers: Peeking at the Peaks. *Annu. Rev. Phys. Chem.* **1998,** *49*, 297-336.

11 De Feyter, S.; De Schryver, F. C., Two-Dimensional Supramolecular Self-Assembly Probed by Scanning Tunneling Microscopy. *Chem. Soc. Rev.* **2003,** *32*, 139-150.

12 MacLeod, J. M.; Rosei, F., Molecular Self-Assembly on Graphene. *Small* **2014,** *10*, 1038-1049.

13 Mali, K. S.; Pearce, N.; De Feyter, S.; Champness, N. R., Frontiers of Supramolecular Chemistry at Solid Surfaces. *Chem. Soc. Rev.* **2017,** *46*, 2520-2542.

14 Gobbi, M.; Orgiu, E.; Samori, P., When 2D Materials Meet Molecules: Opportunities and Challenges of Hybrid Organic/Inorganic van der Waals Heterostructures. *Adv. Mater.* **2018,** *DOI: 10.1002/adma.201706103*.

15 de la Rosa, C. J. L.; Phillipson, R.; Teyssandier, J.; Adisoejoso, J.; Balaji, Y.; Huyghebaert, C.; Radu, I.; Heyns, M.; De Feyter, S.; De Gendt, S., Molecular Doping of MoS2 Transistors by Self-Assembled Oleylamine Networks. *Appl. Phys. Lett.* **2016,** *109*.

16 Phillipson, R.; de la Rosa, C. J. L.; Teyssandier, J.; Walke, P.; Waghray, D.; Fujita, Y.; Adisoejoso, J.; Mali, K. S.; Asselierghs, I.; Huyghebaert, C*., et al.*, Tunable Doping of Graphene by Using Physisorbed Self-Assembled Networks. *Nanoscale* **2016,** *8*, 20017-20026.

17 Fu, C. Y.; Lin, H. P.; Macleod, J. M.; Krayev, A.; Rosei, F.; Perepichka, D. F., Unravelling the Self-Assembly of Hydrogen Bonded NDI Semiconductors in 2D and 3D. *Chem. Mater.* **2016,** *28*, 951-961.

18 Cao, H.; Minoia, A.; De Cat, I.; Seibel, J.; Waghray, D.; Li, Z.; Cornil, D.; Mali, K. S.; Lazzaroni, R.; Dehaen, W.*, et al.*, Hierarchical Self-Assembly of Enantiopure and Racemic Helicenes at the Liquid/Solid Interface: From 2D to 3D. *Nanoscale* **2017,** *9*, 18075-18080.

19 Iritani, K.; Tahara, K.; De Feyter, S.; Tobe, Y., Host-Guest Chemistry in Integrated Porous Space Formed by Molecular Self-Assembly at Liquid-Solid Interfaces. *Langmuir* **2017,** *33*, 4601-4618.

20 Alaboson, J. M. P.; Sham, C.-H.; Kewalramani, S.; Emery, J. D.; Johns, J. E.; Deshpande, A.; Chien, T.; Bedzyk, M. J.; Elam, J. W.; Pellin, M. J.*, et al.*, Templating Sub-10 nm Atomic Layer Deposited Oxide Nanostructures on Graphene Via One-Dimensional Organic Self-Assembled Monolayers. *Nano Lett.* **2013,** *13*, 5763-5770.

21 Elinski, M. B.; Menard, B. D.; Liu, Z. T.; Batteas, J. D., Adhesion and Friction at Graphene/Self-Assembled Monolayer Interfaces Investigated by Atomic Force Microscopy. *J. Phys. Chem. C* **2017,** *121*, 5635-5641.

22 Bang, J. J.; Rupp, K. K.; Russell, S. R.; Choong, S. W.; Claridge, S. A., Sitting Phases of Polymerizable Amphiphiles for Controlled Functionalization of Layered Materials. *J. Am. Chem. Soc.* **2016,** *138*, 4448-4457.

23 Villarreal, T. A.; Russell, S. R.; Bang, J. J.; Patterson, J. K.; Claridge, S. A., Modulating Wettability of Layered Materials by Controlling Ligand Polar Headgroup Dynamics. *J. Am. Chem. Soc.* **2017,** *139*, 11973-11979.

24 Choong, S. W.; Russell, S. R.; Bang, J. J.; Patterson, J. K.; Claridge, S. A., Sitting Phase Monolayers of Polymerizable Phospholipids Create Dimensional, Molecular-Scale Wetting Control for Scalable Solution Based Patterning of Layered Materials. *ACS Appl. Mater. Interf.* **2017,** *9*, 19326-19334.

25 Russell, S. R.; Davis, T. C.; Bang, J. J.; Claridge, S. A., Spectroscopic Metrics for Alkyl Chain Ordering in Lying-Down Monolayers of Diynoic Acids on Graphene. *Chem. Mater.* **2018,** *30*, 2506-2514.

26 Hibshman, H. J., *Ind. Eng. Chem. Res.* **1950,** *42*, 1310-1314.

27 Breshchenko, E. M., *Khimiya Technol. Topl.* **1957,** *9*, 32.

28 Groszek, A. J., Preferential Adsorption of Normal Hydrocarbons on Cast Iron. *Nature* **1962,** *196*, 531-533.

29 Groszek, A. J., Preferential Adsorption of Long-Chain Normal Paraffins on MoS2 Ws2 and Graphite from N-Heptane. *Nature* **1964,** *204*, 680.

30 Binnig, G.; Rohrer, H., Scanning Tunneling Microscopy. *Helv. Phys. Acta* **1982,** *55*, 726-735.

31 McGonigal, G. C.; Bernhardt, R. H.; Thomson, D. J., Imaging Alkane Layers at the Liquid Graphite Interface with the Scanning Tunneling Microscope. *Appl. Phys. Lett.* **1990,** *57*, 28-30.

32 Rabe, J. P.; Buchholz, S., Commensurability and Mobility in 2-Dimensional Molecular-Patterns on Graphite. *Science* **1991,** *253*, 424-427.

33 Cyr, D. M.; Venkataraman, B.; Flynn, G. W., STM Investigations of Organic Molecules Physisorbed at the Liquid-Solid Interface. *Chem. Mater.* **1996,** *8*, 1600-1615.

34 Mann, J. A.; Rodriguez-Lopez, J.; Abruna, H. D.; Dichtel, W. R., Multivalent Binding Motifs for the Noncovalent Functionalization of Graphene. *J. Am. Chem. Soc.* **2011,** *133*, 17614-17617.

35 Gatti, R.; MacLeod, J. M.; Lipton-Duffin, J. A.; Moiseev, A. G.; Perepichka, D. F.; Rosei, F., Substrate, Molecular Structure, and Solvent Effects in 2D Self-Assembly Via Hydrogen and Halogen Bonding. *J. Phys. Chem. C* **2014,** *118*, 25505-25516.

36 Rao, M. R.; Fang, Y.; De Feyter, S.; Perepichka, D. F., Conjugated Covalent Organic Frameworks Via Michael Addition-Elimination. *J. Am. Chem. Soc.* **2017,** *139*, 2421-2427.

37 Colson, J. W.; Woll, A. R.; Mukherjee, A.; Levendorf, M. P.; Spitler, E. L.; Shields, V. B.; Spencer, M. G.; Park, J.; Dichtel, W. R., Oriented 2D Covalent Organic Framework Thin Films on Single-Layer Graphene. *Science* **2011,** *332*, 228-231.

38 Grim, P. C. M.; De Feyter, S.; Gesquiere, A.; Vanoppen, P.; Rucker, M.; Valiyaveettil, S.; Moessner, G.; Mullen, K.; De Schryver, F. C., Submolecularly Resolved Polymerization of Diacetylene Molecules on the Graphite Surface Observed with Scanning Tunneling Microscopy. *Angew. Chem., Int. Ed.* **1997,** *36*, 2601-2603.

39 Okawa, Y.; Aono, M., Linear Chain Polymerization Initiated by a Scanning Tunneling Microscope Tip at Designated Positions. *J. Chem. Phys.* **2001,** *115*, 2317-2322.

40 Okawa, Y.; Akai-Kasaya, M.; Kuwahara, Y.; Mandal, S. K.; Aono, M., Controlled Chain Polymerisation and Chemical Soldering for Single-Molecule Electronics. *Nanoscale* **2012,** *4*, 3013-3028.

41 Seher, A., Die Konstitution Der Isan- Und Isanolsaure. *Eur. J. Org. Chem.* **1954,** *589*, 222-226.

42 Bohlmann, F., Struktur Und Reaktionsfiihigkeit Der Acetylen-Bindung. *Angew. Chem.* **1957,** *69*, 82-86.

43 Wegner, G., Topochemical Reactions of Monomers with Conjugated Triple Bonds .I. Polymerization of 2.4-Hexadiyn-1.6-Diols Derivatives in Crystalline State. *Z. Naturforsch., B: J. Chem. Sci.* **1969,** *B 24*, 824-826.

44 Tieke, B.; Graf, H. J.; Wegner, G.; Naegele, B.; Ringsdorf, H.; Banerjie, A.; Day, D.; Lando, J. B., Polymerization of Monolayer and Multilayer Forming Diacetylenes. *Colloid Polym. Sci.* **1977,** *255*, 521-531.

45 Baughman, R. H., Solid-State Polymerization of Diacetylenes. *J. Appl. Phys.* **1972,** *43*, 4362-4370.

46 Chance, R. R.; Patel, G. N.; Turi, E. A.; Khanna, Y. P., Energetics of Thermal Polymerization of a Diacetylene Crystal. *J. Am. Chem. Soc.* **1978,** *100*, 1307-1309.

47 Tieke, B.; Wegner, G., Quantum Yield of Topochemical Photo-Polymerization of Diacetylenes in Multilayers. *Makromol. Chem.* **1978,** *179*, 1639-1642.

48 Wegner, G., Topochemical Reactions of Monomers with Conjugated Triple Bonds .3. Solid-State Reactivity of Derivatives of Diphenyldiacetylene. *J. Polym. Sci., Part B: Polym. Lett.* **1971,** *9*, 133-144.

49 Bloor, D.; Koski, L.; Stevens, G. C.; Preston, F. H.; Ando, D. J., Solid-State Polymerization of Bis-(Para-Toluene Sulfonate) of 2,4-Hexadiyne-1,6-Diol .1. X-Ray-Diffraction and Spectroscopic Observations. *J. Mater. Sci.* **1975,** *10*, 1678-1688.

50 Baughman, R. H.; Witt, J. D.; Yee, K. C., Raman Spectral Shifts Relevant to Electron Delocalization in Polydiacetylenes. *J. Chem. Phys.* **1974,** *60*, 4755-4759.

51 Schott, M., The Colors of Polydiacetylenes: A Commentary. *J. Phys. Chem. B* **2006,** *110*, 15864-15868.
52 Tieke, B.; Wegner, G.; Naegele, D.; Ringsdorf, H., Polymerization of Tricosa-10,12-Diynoic Acid in Multilayers. *Angew. Chem., Int. Ed. Engl.* **1976,** *15*, 764-765.
53 Bader, H.; Dorn, K.; Hupfer, B.; Ringsdorf, H., Polymeric Monolayers and Liposomes as Models for Biomembranes - How to Bridge the Gap between Polymer Science and Membrane Biology. *Adv. Polym. Sci.* **1985,** *64*, 1-62.
54 Jelinek, R.; Rigenberg, M., Polydiacetylenes - Recent Molecular Advances and Applications. *RSC Adv.* **2013,** *3*, 21192-21201.
55 Hub, H. H.; Hupfer, B.; Koch, H.; Ringsdorf, H., Polyreactions in Ordered Systems .20. Polymerizable Phospholipid Analogs - New Stable Biomembrane and Cell Models. *Angew. Chem., Int. Ed. Engl.* **1980,** *19*, 938-940.
56 Johnston, D. S.; Sanghera, S.; Pons, M.; Chapman, D., Phospholipid Polymers - Synthesis and Spectral Characteristics. *Biochim. Biophys. Act.* **1980,** *602*, 57-69.
57 Obrien, D. F.; Whitesides, T. H.; Klingbiel, R. T., The Photo-Polymerization of Lipid-Diacetylenes in Bimolecular-Layer Membranes. *J. Polym. Sci., Part C: Polym. Lett.* **1981,** *19*, 95-101.
58 O'Brien, D. F.; Armitage, B.; Benedicto, A.; Bennett, D. E.; Lamparski, H. G.; Lee, Y. S.; Srisiri, W.; Sisson, T. M., Polymerization of Preformed Self Organized Assemblies. *Acc. Chem. Res.* **1998,** *31*, 861-868.
59 Rabe, J. P.; Buchholz, S.; Askadskaya, L., Scanning Tunneling Microscopy of Several Alkylated Molecular Moieties in Monolayers on Graphite. *Synth. Met.* **1993,** *54*, 339-349.
60 Akai-Kasaya, M.; Shimizu, K.; Watanabe, Y.; Saito, A.; Aono, M.; Kuwahara, Y., Electronic Structure of a Polydiacetylene Nanowire Fabricated on Highly Ordered Pyrolytic Graphite. *Phys. Rev. Lett.* **2003,** *91*, 255501.
61 Okawa, Y.; Takajo, D.; Tsukamoto, S.; Hasegawa, T.; Aono, M., Atomic Force Microscopy and Theoretical Investigation of the Lifted-up Conformation of Polydiacetylene on a Graphite Substrate. *Soft Matt.* **2008,** *4*, 1041-1047.
62 Mandal, S. K.; Okawa, Y.; Hasegawa, T.; Aono, M., Rate-Determining Factors in the Chain Polymerization of Molecules Initiated by Local Single-Molecule Excitation. *ACS Nano* **2011,** *5*, 2779-2786.
63 Wegner, G., Topochemical Reactions of Monomers with Conjugated Triple-Bonds .4. Polymerization of Bis-(Para-Toluene Sulfonate) of 2.4-Hexadiin-1.6-Diol. *Makromol. Chem.* **1971,** *145*, 85-94.
64 Giridharagopal, R.; Kelly, K. F., Substrate-Dependent Properties of Polydiacetylene Nanowires on Graphite and MoS_2. *ACS Nano* **2008,** *2*, 1571-1580.
65 Neuheuser, T.; Hess, B. A.; Reutel, C.; Weber, E., Ab-Initio Calculations of Supramolecular Recognition Modes - Cyclic Versus Noncyclic Hydrogen-Bonding in the Formic-Acid Formamide System. *J. Phys. Chem.* **1994,** *98*, 6459-6467.
66 Laibinis, P. E.; Whitesides, G. M.; Allara, D. L.; Tao, Y. T.; Parikh, A. N.; Nuzzo, R. G., Comparison of the Structures and Wetting Properties of Self-Assembled Monolayers of Normal Alkanethiols on the Coinage Metal Surfaces, Cu, Ag, Au. *J. Am. Chem. Soc.* **1991,** *113*, 7152-7167.
67 Lee, T. R.; Carey, R. I.; Biebuyck, H. A.; Whitesides, G. M., The Wetting of Monolayer Films Exposing Ionizable Acids and Bases. *Langmuir* **1994,** *10*, 741-749.
68 Fears, K. P.; Creager, S. E.; Latour, R. A., Determination of the Surface pK of Carboxylic- and Amine-Terminated Alkanethiols Using Surface Plasmon Resonance Spectroscopy. *Langmuir* **2008,** *24*, 837-843.
69 Brockman, H., Dipole Potential of Lipid-Membranes. *Chem. Phys. Lipids* **1994,** *73*, 57-79.
70 Lee, A. G., Lipid-Protein Interactions in Biological Membranes: A Structural Perspective. *Biochim. Biophys. Act. - Biomembr.* **2003,** *1612*, 1-40.
71 Killian, J. A., Hydrophobic Mismatch between Proteins and Lipids in Membranes. *Biochim. Biophys. Acta, Rev. Biomembr.* **1998,** *1376*, 401-416.
72 Palsdottir, H.; Hunte, C., Lipids in Membrane Protein Structures. *Biochim. Biophys. Act. - Biomembr.* **2004,** *1666*, 2-18.
73 Strandberg, E.; Killian, J. A., Snorkeling of Lysine Side Chains in Transmembrane Helices: How Easy Can It Get? *FEBS Lett.* **2003,** *544*, 69-73.
74 Israelachvili, J. N., *Intermolecular and Surface Forces*. 3rd ed.; Elsevier: Waltham, MA, 2011.
75 Yin, S.; Wang, C.; Qiu, X.; Xu, B.; Bai, C., Theoretical Study of the Effects of Intermolecular Interactions in Self-Assembled Long-Chain Alkanes Adsorbed on Graphite Surface. *Surf. Interf. Anal.* **2001,** *32*, 248-252.
76 Drelich, J.; Wilbur, J. L.; Miller, J. D.; Whitesides, G. M., Contact Angles for Liquid Drops at a Model Heterogeneous Surface Consisting of Alternating and Parallel Hydrophobic Hydrophilic Strips. *Langmuir* **1996,** *12*, 1913-1922.
77 Checco, A.; Gang, O.; Ocko, B. M., Liquid Nanostripes. *Phys. Rev. Lett.* **2006,** *96*.
78 Jansen, H. P.; Sotthewes, K.; van Swigchem, J.; Zandvliet, H. J. W.; Kooij, E. S., Lattice Boltzmann Modeling of Directional Wetting: Comparing Simulations to Experiments. *Phys. Rev. E* **2013,** *88*, 013008.
79 Love, J. C.; Estroff, L. A.; Kriebel, J. K.; Nuzzo, R. G.; Whitesides, G. M., Self-Assembled Monolayers of Thiolates on Metals as a Form of Nanotechnology. *Chem. Rev.* **2005,** *105*, 1103-1169.
80 Saavedra, H. M.; Mullen, T. J.; Zhang, P. P.; Dewey, D. C.; Claridge, S. A.; Weiss, P. S., Hybrid Strategies in Nanolithography. *Rep. Prog. Phys.* **2010,** *73*.
81 Lee, S. L.; Chi, C. Y. J.; Huang, M. J.; Chen , C. H.; Li, C. W.; Pati, K.; Liu, R. S., Shear-Induced Long-Range Uniaxial Assembly of Polyaromatic Monolayers at Molecular Resolution. *J. Am. Chem. Soc.* **2008,** *130*, 10454-10455.
82 Lee, S.-L.; Yuan, Z.; Chen, L.; Mali, K. S.; Muellen, K.; De Feyter, S., Forced to Align: Flow-Induced Long-Range Alignment of Hierarchical Molecular Assemblies from 2D to 3D. *J. Am. Chem. Soc.* **2014,** *136*, 4117-4120.
83 Blodgett, K. B., Monomolecular Films of Fatty Acids on Glass. *J. Am. Chem. Soc.* **1934,** *56*, 495-495.
84 Langmuir, I.; Schaefer, V. J., Activities of Urease and Pepsin Monolayers. *J. Am. Chem. Soc.* **1938,** *60*, 1351-1360.
85 Honig, E. P.; Hengst, J. H. T.; Denengel, D., Langmuir-Blodgett Deposition Ratios. *J. Colloid Interface Sci.* **1973,** *45*, 92-102.

86 Chen, X.; Lenhert, S.; Hirtz, M.; Lu, N.; Fuchs, H.; Chi, L., Langmuir-Blodgett Patterning: A Bottom-up Way to Build Mesostructures over Large Areas. *Acc. Chem. Res.* **2007,** *40*, 393-401.

87 Li, Z.; Wang, Y.; Kozbial, A.; Shenoy, G.; Zhou, F.; McGinley, R.; Ireland, P.; Morganstein, B.; Kunkel, A.; Surwade, S. P.*, et al.*, Effect of Airborne Contaminants on the Wettability of Supported Graphene and Graphite. *Nat. Mater.* **2013,** *12*, 925-931.

88 Hayes, T. R.; Bang, J. J.; Davis, T. C.; Peterson, C. F.; McMillan, D. G.; Claridge, S. A., Multimicrometer Noncovalent Monolayer Domains on Layered Materials through Thermally Controlled Langmuir-Schaefer Conversion for Noncovalent 2D Functionalization. *ACS Appl. Mater. Interf.* **2017,** *9*, 36409–36416.

89 Davis, T. C.; Bang, J. J.; Brooks, J. T.; McMillan, D. G.; Claridge, S. A., Hierarchical Noncovalent Functionalization of 2D Materials by Controlled Langmuir-Schaefer Conversion. *Langmuir* **2018,** *34*, 1353-1362.

90 Bang, J. J.; Porter, A. G.; Davis, T. C.; Hayes, T. R.; Claridge, S. A., Spatially Controlled Noncovalent Functionalization of 2D Materials Based on Molecular Architecture *Langmuir* **2018,** *ASAP. DOI: 10.1021/acs.langmuir.8b00553*.

91 Doudevski, I.; Hayes, W. A.; Schwartz, D. K., Submonolayer Island Nucleation and Growth Kinetics During Self-Assembled Monolayer Formation. *Phys. Rev. Lett.* **1998,** *81*, 4927-4930.

92 Duevel, R. V.; Corn, R. M., Amide and Ester Surface Attachment Reactions for Alkanethiol Monolayers at Gold Surfaces as Studied by Polarization Modulation Fourier-Transform Infrared-Spectroscopy. *Anal. Chem.* **1992,** *64*, 337-342.

93 Blaudez, D.; Castano, S.; Desbat, B., PM-IRRAS at Liquid Interfaces. In *Biointerface Characterization by Advanced IR Spectroscopy*, Pradier, C.-M.; Chabal, Y. J., Eds. Elsevier: 2011.

94 Fu, C. Y.; Beldon, P. J.; Perepichka, D. F., H-Bonding Control of Supramolecular Ordering of Diketopyrrolopyrroles. *Chem. Mater.* **2017,** *29*, 2979-2987.

95 Mezour, M. A.; Choueiri, R. M.; Lukoyanova, O.; Lennox, R. B.; Perepichka, D. F., Hydrogen Bonding vs. Molecule-Surface Interactions in 2D Self-Assembly of C60 Fullerenecarboxylic Acids. *Nanoscale* **2016,** *8*, 16955-16962.

96 Russell, S. R.; Claridge, S. A., Peptide Interfaces with Graphene: An Emerging Intersection of Analytical Chemistry, Theory, and Materials. *Anal. Bioanal. Chem.* **2016,** *408*, 2649-2658.

97 Mezour, M. A.; Voznyy, O.; Sargent, E. H.; Lennox, R. B.; Perepichka, D. F., Controlling C-60 Organization through Dipole-Induced Band Alignment at Self-Assembled Monolayer Interfaces. *Chem. Mater.* **2016,** *28*, 8322-8329.

98 Wei, Y. H.; Tong, W. J.; Zimmt, M. B., Self-Assembly of Patterned Monolayers with Nanometer Features: Molecular Selection Based on Dipole Interactions and Chain Length. *J. Am. Chem. Soc.* **2008,** *130*, 3399-3405.

99 Verstraete, L.; Hirsch, B. E.; Greenwood, J.; De Feyter, S., Confined Polydiacetylene Polymerization Reactions for Programmed Length Control. *Chem. Comm.* **2017,** *53*, 4207-4210.

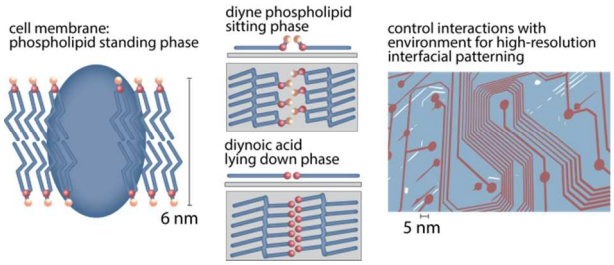

Lessons can be drawn from cell membranes in controlling noncovalent functionalization of 2D materials to optimize interactions with the environment.

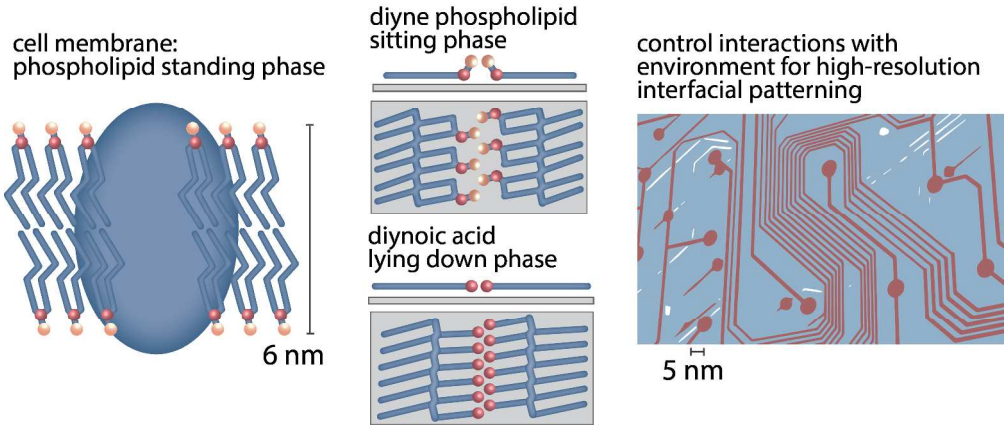
cell membrane:
phospholipid standing phase
6 nm
diyne phospholipid
sitting phase
diynoic acid
lying down phase
control interactions with
environment for high-resolution
interfacial patterning
5 nm